The Viscosity and Thermal Conductivity Coefficients of Dilute Nitrogen and Oxygen*

H. J. M. Hanley and James F. Ely†

Cryogenics Division, National Bureau of Standards, Boulder, Colorado 80302

The viscosity and thermal conductivity coefficients of dilute oxygen and nitrogen are discussed and tables of values are presented for temperatures between 80 and 2000 K. The oxygen viscosity tables are estimated to be accurate to two percent for temperatures up to 400 K and four percent above that temperature; the nitrogen viscosity tables are estimated to be reliable to one percent in the range 100–1000 K, increasing to two percent above 1000 K and below 100 K. The error assigned to the thermal conductivity is three percent below 400 K and five percent above 400 K for both gases. The tables were calculated from the appropriate kinetic theory equations using the m–6–8 model potential with nonspherical contributions. The approximations to the equations are discussed. It is emphasized that the available data for oxygen viscosity are generally poor and that the thermal conductivity data for both oxygen and nitrogen cannot be considered reliable at high temperatures. No oxygen data exist for temperatures above 1500 K.

Key words: Critically evaluated data; dilute polyatomic gas; kinetic theory of polyatomic molecules; m–6–8 potential; nitrogen; nonspherical interactions; oxygen; second virial coefficient; thermal conductivity coefficient; thermal diffusion factor; viscosity coefficient.

1. Introduction

In a recent publication (referred to as I) [1][1], the transport properties of the heavy rare gases were discussed and tables of the viscosity and thermal conductivity coefficients were presented. The correlation attempted to ensure that these two properties were mutually consistent for a given gas and were also consistent with other independent properties of the same gas. It was stressed that the correlation was weighted to favor the more recent viscosity data (i.e., reported since about 1968) which have been shown to be generally more reliable than corresponding older data.

In this paper the correlation procedure is extended to cover the transport properties of two nonpolar polyatomic gases, nitrogen and oxygen. Tabulated viscosity and thermal conductivity coefficients are presented for the temperature range 80–2000 K.

2. Data

We have some remarks on the nitrogen and oxygen data but experimental techniques are not discussed. References on experimental techniques are listed in I.

Viscosity

A conclusion from I was that the available rare gas viscosity data are generally satisfactory, for argon especially. The conclusion was supported by experimental arguments, e.g., by comparing results obtained from different techniques—the oscillating disc, the oscillating crystal and the capillary flow techniques, and by semi-theoretical arguments showing that the intermolecular potential function, selected to correlate viscosity data via kinetic theory, can correlate other independent properties without parameter adjustment. Since most of the sources responsible for the rare gas data report data for nitrogen, one can initially assume that these nitrogen viscosities are probably reliable. We refer specifically to the work of Kestin [2], Smith [3, 4], Gracki [5], and Guevara [6] whose data will form the basis for the nitrogen correlation (see table 1).[2]

Unfortunately, the data base for an oxygen correlation cannot be considered satisfactory. Several data sets are in the literature, but viscosities above room temperature are due to Trautz [11] and to Raw and Ellis [12]. The data of Trautz, reported 40 years ago, have to be regarded as seriously in error at the higher temperatures [13] and those of reference [12] are not internally consistent [14]. The published data for viscosities below room temperature are mainly due to Johnston [8] and are probably slightly too high.[3]

In order to present tabulated viscosities for oxygen which take into account the very probable errors in the data, we have had to make adjustments to the data based on the following observation: Figure 1 shows a curve giving the deviations between recent and corresponding older viscosity coefficients for several gases: argon, helium, methane, nitrogen, and air. The recent work is represented by Smith [3, 4, 15, 16], Guevara [6], and Kestin [2] while the older work is represented by

[1] Numbers in brackets refer to the references.

* Work carried out at the National Bureau of Standards under the sponsorship of the Office of Standard Reference Data.

† NRC–NBS Postdoctoral Research Associate. Present address: Department of Chemical Engineering, Rice University, Houston, Tx. 77001.

[2] Tables have been placed at the end of this paper.

[3] It was noted in I that the work of references [2–6] reflects the significant improvement in the state-of-the-art of viscosity measurement of the last six years or so. In fact, it is commonly accepted that many viscosities published prior to that time are systematically in error outside a temperature range of ~250 to ~400 K. In particular, at high temperatures, the modern experiments give viscosity coefficients which tend to be higher than their older equivalents; corresponding data differ by 1–10 percent in the range 400 to 2000 K—the difference increasing with temperature. At low temperatures, the discrepancy is not so noticeable but the modern data tend to be generally lower by 1/2–2 percent—the difference increasing as the temperature decreases.

Johnston [8, 17] and Trautz [18]. The curve is smoothed and schematic (see reference [14] for more discussion) but it illustrates that, to a first approximation, the discrepancy between the two representative sets of data does *not* depend on the gas considered but depends only on the temperature.

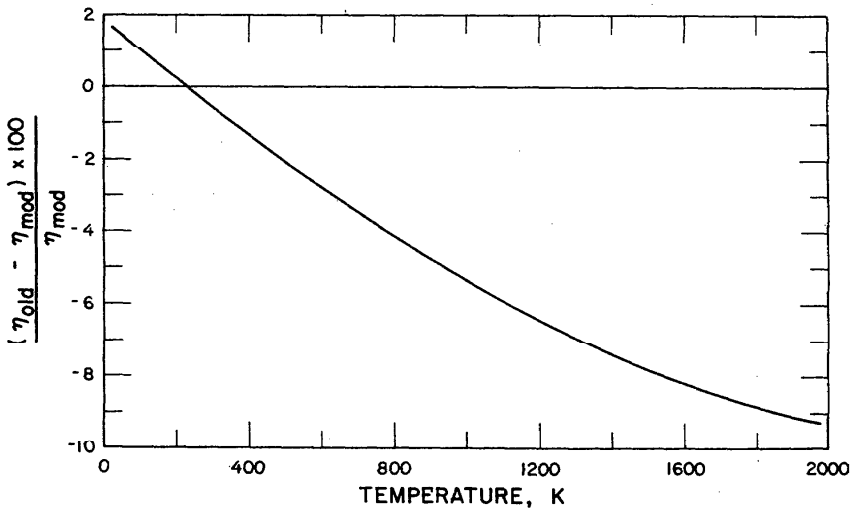

FIGURE 1. Schematic diagram illustrating differences between old and recent viscosity data for the gases argon, helium, methane, nitrogen, and air. To a first approximation the difference is independent of the gas, reflected by the fact that a single curve is shown in the figure.

Accordingly, *we have adjusted* the oxygen viscosity data from references [8] and [11] (see also [18]) by the percentage indicated in figure 1 at the proper temperature. The adjusted data are listed in table 2 and, together with much more limited results from references [7] and [19–22], form the basis for the oxygen correlation.

Thermal Conductivity

Two remarks were made in I concerning thermal conductivity data. The first commented on the experimental problems in measuring the coefficient. Only two apparatuses, the parallel plate and the concentric cylinder devices, seem capable of measuring the thermal conductivity coefficient with high accuracy and only very few authors can claim to have, on experimental grounds, reliable results. Generally, therefore, thermal conductivity values are imprecise. (Very recent advances with a transient hot wire technique [23] indicate that considerable improvements are possible in measuring the conductivity over a wide range of density and temperature.)

The second remark concerned the simple relationship that exists for monatomic gases between the viscosity and thermal conductivity coefficients: If reliable viscosity data are available, the thermal conductivity coefficient can generally be predicted to an accuracy better than it can presently be measured. In other words, thermal conductivity results were used in I more to check the correlation procedure than as primary input data.

For the gases of interest here, oxygen and nitrogen the first remark is directly relevant but the second requires modification: the thermal conductivity coefficient can be calculated given the viscosity but the relationship is more complicated and involves several assumptions which are difficult to assess. Nevertheless, the overall accuracy of the thermal conductivity data in the literature is such that an empirical correlation of these data would not give tabular values to better than 5–10 percent. In our judgment, a correlation based on calculated values would represent the data to within this accuracy and the values would be consistent with the corresponding viscosity coefficients (to within the theoretical assumptions). Hence, as for the rare gases, thermal conductivity data for nitrogen and oxygen are not used as primary information for the purposes of this paper.

Data from the following sources were selected to compare the calculations with experiment: nitrogen, references [24–27]; oxygen, references [24, 35, 38–45] (table 1). For a given gas, the data from different sources agree to within about 5 percent in the temperature range ~ 100–1000 K. At very low temperatures and at temperatures above 1000 K, the agreement becomes worse; about 10 percent at 100 K and about 15 percent at 1500 K, for example. From an experimental analysis of the experimental techniques involved, the data from reference [25] (concentric cylinder apparatus), references [30 and 37] (parallel plate), and reference [29] (transient hot wire) can be considered the more reliable although it is suspected that the data from references [30] and [37] may be erroneous at high densities due to convection problems in the measurement. Also the results

from references [26] and [27] for gases other than oxygen or nitrogen—specifically for the rare gases from [27] and carbon dioxide from [26]—seem reliable. We note, however, that data above 1500 K are very scarce and that none of the above mentioned references apply to oxygen.

Compilations of references for the transport properties of oxygen and nitrogen, including those not discussed here are given in references [14, 46, 47, and 48].

3. Kinetic Theory Equations

The kinetic theory of dilute monatomic gases leads to expressions for the viscosity and thermal conductivity coefficients which form the basis for a tabulation of values provided a suitable intermolecular potential, Φ, is available. The spherically symmetric m–6–8 was used in I:

$$\Phi_s(r) = \frac{\epsilon}{m-6}[6+2\gamma]\left(\frac{r_m}{r}\right)^m - \frac{\epsilon}{m-6}[m-\gamma(m-8)]\left(\frac{r_m}{r}\right)^6 - \gamma\epsilon\left(\frac{r_m}{r}\right)^8, \quad (1)$$

where $\Phi_s(r_m) = -\epsilon$. For later use, we define a distance parameter σ by $\Phi_s(\sigma) = 0$. The potential has four adjustable parameters; m, γ, ϵ, and r_m (or σ).

The kinetic theory of polyatomic gases has been discussed by several authors [49–51] and formal expressions for the transport coefficients have been presented which correspond to first order Chapman-Enskog solutions of the Boltzmann equation. Mason and Monchick and their co-workers have discussed these very complex equations in considerable detail [52–55] and proposed workable and more practical adaptations. Their equations are the foundation for the correlations presented here. Since they are not as familiar as the corresponding equations for the monatomic gases, the necessary approximations are summarized.

Two major complications are introduced when kinetic theory is extended to polyatomic gases: a) the molecular collisions are inelastic, b) the intermolecular interactions will be angle dependent, i.e., will depend on the relative orientations of the colliding molecules.

3.1. Inelastic Collisions

Consider first the viscosity. The formal expression for this coefficient, η, is

$$\eta = \frac{5}{16}\frac{(\pi mkT)^{1/2}}{\pi\sigma^2\langle\Omega^{(2,2)*}\rangle}, \quad (2)$$

where the collision integral is given by

$$\langle\Omega^{(2,2)*}\rangle = \frac{A_1^{-1}A_2^{-1}}{T^{*2}}\int [g^{*4}(1-\cos^2\chi) - \frac{2T^*}{3}(g'^{*2}+g^{*2}\sin^2\chi)\Delta\epsilon^o] \exp[-\epsilon_1^o-\epsilon_2^o-g^{*2}/T^*]b^*db^*g^{*3}dg^*d\omega_1d\omega_2, \quad (3)$$

where $A_j = \int \exp(-\epsilon_j^o)\, d\omega_j$, $(j = 1, 2)$. The angular brackets will be explained shortly.

In the above equations, m is the mass of a molecule, k Boltzmann's constant and T the temperature in kelvin. We have discussed the reduced quantities in I. Given an energy parameter ϵ and distance parameter σ defined by equation (1), $g^*[= mg/4\epsilon]$ is the reduced relative velocity of molecules 1 and 2 before a collision and g'^* the reduced relative velocity after a collision, b^* is reduced impact parameter $[= b/\sigma]$, and T^* the reduced temperature $[= T/(\epsilon/k)]$. The angle χ, is the deflection angle defined by equation (4) of I.

Equation (3) is seen to be similar to the viscosity collision integral for an elastic collision [equation (6) of I] except that the internal energy of the molecules is now included, viz., if E_i is the energy of molecule i due to internal degrees of freedom with coordinates and momenta about the center of mass of molecule i given by ω_i, $\epsilon_i^o = E_i/\epsilon$ and $\Delta\epsilon^o = \epsilon_1^{o\prime} + \epsilon_2^{o\prime} - \epsilon_1^o - \epsilon_2^o = g^{*2} - g'^{*2}$, where the primes refer to quantities after a collision.

The polyatomic gas viscosity expression is thus formally close to that for the monatomic gas. The corresponding expression for the thermal conductivity coefficient is more involved, however. Not only are the collision integrals more complex, but internal energy is transferred through the gas by a diffusion mechanism. Further, the formal derivation of the conductivity expression includes a contribution directly proportional to powers of $\Delta\epsilon^o$. Experience has shown that this contribution should not be neglected unless $\Delta\epsilon^o$ is very close to zero. Fortunately Monchick and Mason [54, 55] have considerably clarified the formal expression by gathering terms and relating the results to macroscopic properties. Specifically the transfer of internal energy is accounted for by an internal diffusion coefficient, D_{int}:

$$\rho D_{\text{int}} = \frac{3}{8}\frac{(\pi mkT)^{1/2}}{\pi\sigma^2\langle\Omega^{(1,1)*}(\text{int})\rangle}, \quad (4)$$

where ρ is the mass density and $\langle\Omega^{(1,1)*}(\text{int})\rangle$ is a collision integral similar to, but not the same as, the collision integral for ordinary diffusion. The energy transfer between translational and internal modes, $\Delta\epsilon^o$, is expressed in terms of a relaxation time τ which turns out to be proportional to $(\Delta\epsilon^o)^{-2}$. In turn a collision number, Z, is defined by the relation

$$Z = \tau/\tau_c, \quad (5)$$

where τ_c is the mean time between collisions. Clearly as $\Delta\epsilon^o \to 0$, $Z \to \infty$. We refer to reference [55] for the

detailed equations for $\langle \Omega^{(1,1)*}(\text{int}) \rangle$ and for τ.

The final equation for the thermal conductivity of a polyatomic gas, λ, is

$$\lambda = \frac{5}{2}\eta\left(\frac{3}{2}\frac{k}{m}\right) + \rho D_{\text{int}} c_v'' - \eta\left(\frac{5}{2} - \frac{\rho D_{\text{int}}}{\eta}\right)\Delta, \quad (6)$$

where c_v'' is the internal specific heat at constant volume and

$$\Delta = \frac{2}{\pi}\frac{c_v''}{Z}\left(\frac{5}{2} - \frac{\rho D_{int}}{\eta}\right)\left[1 + \frac{2}{\pi Z}\left(\frac{5}{3}\frac{mc_v''}{k} + \frac{\rho D_{\text{int}}}{\eta}\right)\right]^{-1}. \quad (7)$$

(in writing these equations, we have assumed that only one internal-translational energy interaction has to be considered; in most cases this would be the rotation-translation.)

It is important to note that equations (2) and (6) are exact and subject only to the first order solution of the Boltzmann equation [56]. However, approximations are necessary in order to apply them in practice:

1. As Monchick and Mason point out [53, 54], on the average the term $\Delta\epsilon^0$ vanishes on integration but, in any case, it is nearly always reasonable to assume that $\Delta\epsilon^0 \ll g^{*2}$. Hence, the collision integrals $\langle \Omega^{(2,2)*} \rangle$ for viscosity and thermal conductivity (and $\langle \Omega^{(1,1)*} \rangle$ for diffusion) approach those derived for elastic collisions, given in I for example. (We have ignored for the moment, the problems associated with nonspherical interactions.)

2. It is impractical to calculate D_{int} at this time and several authors have discussed means to write D_{int} in terms of obtainable quantities. We refer to the paper of Sandler [56], for example. The simplest approach is to set D_{int} equal to D_{11}, the coefficient of self-diffusion for elastic collisions. This definitely is an approximation but comparisons of the thermal conductivity coefficient between theory and experiment with more elaborate forms for D_{int} are inconclusive because experimental thermal conductivity data are too imprecise. Therefore, we will use D_{11} for D_{int}.

3. The equation for λ will be truncated to first order in $1/Z$.

To summarize, the equations for the viscosity and thermal conductivity for a polyatomic gas used in this paper are

$$\eta = \frac{5}{16}\frac{(\pi mkT)^{1/2}}{\pi\sigma^2\langle \Omega^{(2,2)*} \rangle} f_\eta, \quad (8)$$

where

$$f_\eta = 1 + \frac{3}{196}\left(\frac{8\langle \Omega^{(2,3)*} \rangle}{\langle \Omega^{(2,2)*} \rangle} - 7\right)^2, \quad (9)$$

$$\lambda = \frac{5}{2}\eta\left(\frac{3}{2}\frac{k}{m}\right) + \rho D_{11} c_v'' - \frac{2c_v''}{\pi Z}\eta\left(\frac{5}{2} - \frac{\rho D_{11}}{\eta}\right)^2, \quad (10)$$

with

$$\rho D_{11} = \frac{5}{8}\frac{(\pi mkT)^{1/2}}{\pi\sigma^2\langle \Omega^{(1,1)*} \rangle} f_D, \quad (11)$$

where

$$f_D = 1 + \frac{(6C^* - 5)^2}{16A^* + 40}, \quad (12)$$

The terms A^* and C^* are combinations of collision integrals:

$$A^* = \langle \Omega^{(2,2)*} \rangle / \langle \Omega^{(1,1)*} \rangle, \quad (13)$$

$$C^* = \langle \Omega^{(1,2)*} \rangle / \langle \Omega^{(1,1)*} \rangle. \quad (14)$$

In these equations, $\langle \Omega^{(l,s)*} \rangle$, (in general l, $s = 1, 2, 3$) are angularly averaged collision integrals.

(We have not been consistent in that the formal equations for polyatomic gases have been presented to the first order Chapman-Enskog solution only but the equations (8) and (11) are written to second order. This assumes therefore, that the viscosity and diffusion equations for a polyatomic gas have the same form as the equations for a monatomic gas, at least to a second order approximation. For a monatomic gas, these coefficients should be calculated with the second order correction.)

3.2. Nonspherical Interactions

The purpose of the bracket notation in equations (8)–(14) is next discussed. Although equations for the transport properties of a polyatomic gas are known, they strictly cannot be used unless provision is made for nonspherical interactions. In other words, when two nonspherical molecules collide the intermolecular force is dependent on the relative orientation—and under these circumstances the dynamics of a binary collision become extremely complex and effectively unsolvable. Mason, et al. have, however, proposed a straightforward alternative [57]. If the relative orientation of of two molecules during the collision is considered fixed, then it can be shown *without approximation* that the collision integrals become the weighted average of the collision integrals evaluated at a fixed orientation. Specifically, writing $\Phi(\theta_1, \theta_2, \varphi, r)$ as the interaction potential for two axially symmetric nonspherical molecules with orientation angles θ_1, θ_2, and φ, defined in the standard way [58], giving equal weight to all possible fixed orientations, the collision integral becomes

$$\langle \Omega^{(l,s)*} \rangle = \frac{1}{\pi}\int_0^\pi \int_0^1 \int_0^1 \Omega^{(l,s)*}\, d(\cos\theta_1)\, d(\cos\theta_2)\, d\varphi. \quad (15)$$

Therefore, we have two extra assumptions to add to those in section 3.1: (a) that the molecules collide with

fixed orientations and (b) that all orientations are equally probable. Beyond stating that these assumptions seem reasonable, it is not clear what degree of approximation they introduce into a numerical calculation of a transport property.

On the basis of these arguments, equations (8) and (10) for the viscosity and thermal conductivity coefficients respectively can be the foundation for tabular values given a suitable potential function. At this stage, however, we should point out that it has been shown [59] that the *m*–6–8 *spherical* potential of equation (1) can correlate the viscosity and thermal conductivity coefficients of oxygen and nitrogen to within experimental error. This implies that the angularly averaged collision integrals of equation (15) cannot be much different from the angle independent integrals, and that the *m*–6–8 potential parameters, selected on the basis that the intermolecular interactions are spherically symmetric, take into account some of the nonspherical characteristics. A similar conclusion would follow if any sufficiently flexible model potential were used. A correlation could be achieved, therefore, without having to compute angle averaged collision integrals. In I, however, it was stressed that the calculations of the viscosity and thermal conductivity coefficients for the monatomic gases were not only mutually consistent but were also consistent with independent properties such as the second virial coefficient. This overall consistency allowed one to minimize the possibility of serious systematic errors in the transport calculations and to have confidence in extrapolating the calculations outside the range of data. One *cannot* obtain this overall consistent picture for polyatomic gases using a spherical potential. A more sophisticated approach, which does not require angle averaged collision integrals, is to consider nonspherical contributions to the potential, but then assume that they do not play a role in the collision integrals and obtain effective spherical potential parameters from a viscosity fit. The complete potential, with these parameters, can then be used to calculate those properties for which nonspherical contributions definitely have to be considered, the second virial coefficient in particular. This procedure has been quite successful [60], but is not sufficient to give a consistent representation of several independent properties of the polyatomic gas. We thought it worthwhile, therefore, to calculate the viscosity and thermal conductivity coefficients as precisely as is practical at this time bearing in mind that a representation of the transport coefficients to within experimental error is required.

4. Calculations

Details of the calculation procedure are discussed in this section.

4.1. The Potential Function

Following our arguments in the previous section, the calculations are based on a model nonspherical potential. In general for polarizable, quadrupolar molecules such as nitrogen and oxygen, the potential will have the form:

$$\Phi_T = \Phi_s(r) + \Phi\,(\text{quadrupole}) + \Phi\,(\text{induced-dipole}) + \Phi\,(\text{shape}) + \Phi\,(\text{anisotropy}).$$

The first term is the spherical contribution—to be represented by the *m*–6–8 in our case—the second term represents the electrostatic interactions of the permanent multipole moments (quadrupoles) and the third term represents the induced-dipole interactions caused by the induction effect of the quadrupole moments. Finally, the last two terms depict the anisotropy in the repulsive and attractive forces, respectively. However, we have chosen to neglect these latter two contributions [60, 61] in our previous work for the following reasons: (1) it is currently impossible to determine independently the parameters for the shape part of the potential and (2) the spherical *m*–6–8 potential yields a very reasonable representation of experimental transport properties [59] and presumably, therefore, anisotropy is at least partially accounted for in the selection of spherical potential parameters, viz., m, γ, σ, and ϵ/k.

The potential, therefore, is given by the formal expression [62]:

$$\Phi_T(r, \boldsymbol{\omega}_1, \boldsymbol{\omega}_2) = \Phi_s(r) + \Phi_{qq}(r, \boldsymbol{\omega}_1, \boldsymbol{\omega}_2) + \Phi_{ii}(r, \boldsymbol{\omega}_1, \boldsymbol{\omega}_2), \tag{16}$$

where

$$\Phi_{qq}(r, \boldsymbol{\omega}_1, \boldsymbol{\omega}_2) = \mathbf{Q}:\mathbf{V}:\mathbf{Q},$$

$$\Phi_{ii}(r, \boldsymbol{\omega}_1, \boldsymbol{\omega}_2) = -\tfrac{1}{2}(\mathbf{U}:\mathbf{Q}) \cdot \boldsymbol{\alpha} \cdot (\mathbf{1} - \boldsymbol{\alpha} \cdot \mathbf{T})^{-1} \cdot (\mathbf{U}:\mathbf{Q}). \tag{17}$$

In equation (16), $\Phi_s(r)$ is the spherical *m*–6–8 given by equation (1). In equation (17), $\boldsymbol{\omega}_1$ and $\boldsymbol{\omega}_2$ denote the sets of angles describing the orientations of the molecules and $\mathbf{T}$, $\mathbf{U}$, and $\mathbf{V}$ are the two-dimensional supermatrices [62, 73] whose components are the dipole-dipole, dipole-quadrupole, and quadrupole-quadrupole interaction tensors. The cartesian components of these tensors are

$$T_{\alpha\beta}(r) = \nabla_\alpha \nabla_\beta (1/r)$$

$$U_{\alpha\beta\gamma}(r) = \nabla_\alpha \nabla_\beta \nabla_\gamma (1/r)$$

and

$$V_{\alpha\beta\gamma\delta}(r) = \nabla_\alpha \nabla_\beta \nabla_\gamma \nabla_\delta (1/r). \tag{18}$$

$\boldsymbol{\alpha}$ is a matrix whose components are the molecular polarizability tensors and $\mathbf{Q}$ is a supervector whose elements are the molecular quadrupole moment tensors

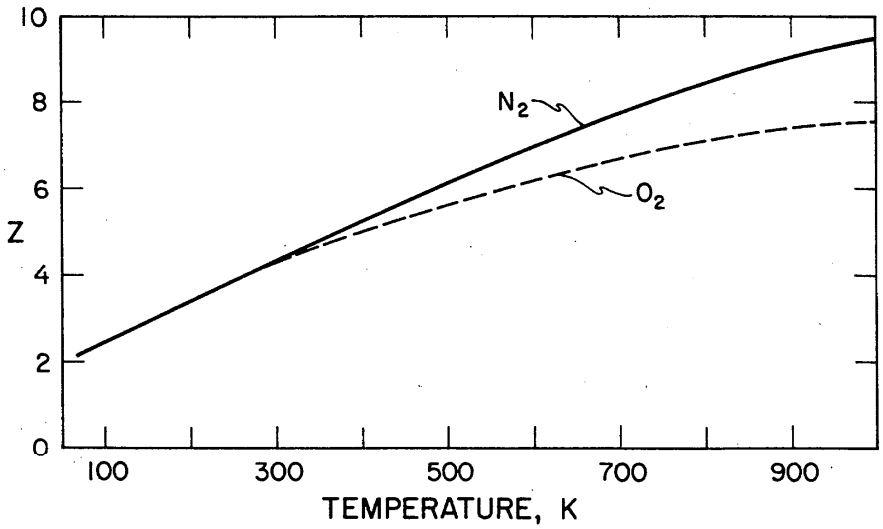

FIGURE 2. Variation of the rotational collision number (Z) for nitrogen and oxygen versus temperature. The curves are based on experimental data summarized in reference [70].

of the different molecules. The elements of these tensors for axial molecules are

$$\alpha_{\beta\gamma}=\bar{\alpha}[(1-\kappa)\delta_{\beta\gamma}+3\kappa\hat{q}_\beta\hat{q}_\gamma],$$

$$Q_{\alpha\beta}=\hat{q}_\alpha\hat{q}_\beta\Theta,$$

where $\bar{\alpha}$ is the mean molecular polarizability, Θ is the scalar quadrupole moment, κ is the polarizability anisotropy and $\mathbf{q}$ is the unit vector along the molecular axis.

It is more convenient to rewrite the nonspherical contributions in terms of the relative orientation angles of the molecular pairs; θ_1, θ_2, φ [see reference 58]. Then one has

$$\Phi_T^*=\Phi_s^*(r)+\frac{\Theta^{*2}}{r^{*5}}F(\theta_1,\theta_2,\varphi)$$

$$-\frac{9}{8}\frac{\bar{\alpha}^*\Theta^{*2}}{r^{*8}}G(\theta_1,\theta_2,\varphi)+O(\bar{\alpha}^2,\Theta^{*2}). \qquad (19)$$

The reduced quantities have been introduced: $\Phi_T^*=\Phi_T/\epsilon$, $\Theta^{*2}=\Theta^2/(\epsilon\sigma^5)$, and $\bar{\alpha}^*=\bar{\alpha}/\sigma^3$, where ϵ and σ are the energy and distance parameters for the spherical m–6–8. The second term of equation (19) represents the quadrupole-quadrupole contribution while the third term represents the first term of the induction contribution from equation (17) neglecting the polarizability anisotropy. We presently feel that it is not necessary to take this contribution to higher order for the transport properties [calculations of the virial coefficients should include terms up to third order in $(\Theta^{*2}, \bar{\alpha}^*)$]. The expressions for F and G are

$$F=\tfrac{3}{4}[1-5\cos^2\theta_1-5\cos^2\theta_2-15\cos^2\theta_1\cos^2\theta_2$$

$$+2(\sin\theta_1\sin\theta_2\cos\varphi-4\cos\theta_1\cos\theta_2)^2], \qquad (20)$$

$$G=\sin^4\theta_1+\sin^4\theta_2+4\cos^4\theta_1+4\cos^4\theta_2. \qquad (21)$$

Parameter Selection

The full potential of equation (19) is considered to have four parameters only, all in the Φ_s term. The other variables—the quadrupole moment and polarizability—are *not* treated as parameters and were obtained from independent sources, as listed in table 3. The m–6–8 parameters for a given gas were determined by the following procedure:

1. Given the spherical collision integrals for the m–6–8 potential [68], initial estimates of m, γ, σ, and ϵ/k were obtained by requiring that the first approximation viscosity equation [with $f_\eta=1$ of equation (8)] fit the selected viscosity data *over the complete temperature range of interest.* Details are given in I and in reference [59]. It should be recalled that this criterion, i.e., requiring the potential to correlate viscosity data over a wide temperature range, is restrictive and can only be achieved with a flexible potential.
2. The value of m so obtained was then considered fixed. Angle averaged collision integrals were then generated from the potential of equation (19) for several values of γ given values of the quadrupole moment, polarizability and the initial estimates of σ and ϵ/k. The calculation procedure is discussed in the Appendix.
3. A value of γ was selected from a further viscosity fit using the angle averaged collision integrals. This fit also led to closer estimates of σ and ϵ/k.
4. Having m and γ, final values of σ and ϵ/k were obtained by fitting the second order viscosity equation to the data. The parameters are summarized in table 3.
5. Tables of $\langle\Omega^{(l,s)*}\rangle$ were thus generated for each gas and are listed in the Appendix.

4.2. Estimation of Z and c_v''

Determination of Z

Several experimental studies on the rotational collision number have been published [68–71]; we refer to figures 2 and 3 of reference [70] for a summary. The variation of Z with temperature for nitrogen and oxygen is shown as figure 2 here. The curves indicate the mean of the data at a given temperature (the experimental uncertainty in Z is about fifty percent). For our calculations, the curves were represented by a table of Z versus temperature and specific values of Z at a given temperature were found by interpolation. For convenience, Z above 1000 K was set at 9.5 and 7.5 for nitrogen and oxygen respectively, and we set $Z=0$ at 0 K for interpolation purposes. It is appreciated that the estimation of Z is very approximate but the experimental data do not warrant a more sophisticated approach.

Determination of c_v''

The total specific heat at constant volume, c_v, has been precisely determined for nitrogen [72] and oxygen [73]. The internal specific heat, c_v'' follows at once.

5. Results and Discussion

Tables for the viscosity and thermal conductivity coefficients for nitrogen and oxygen were generated from equations (8) and (10) as a function of temperature and the results are presented as tables 4 and 5.

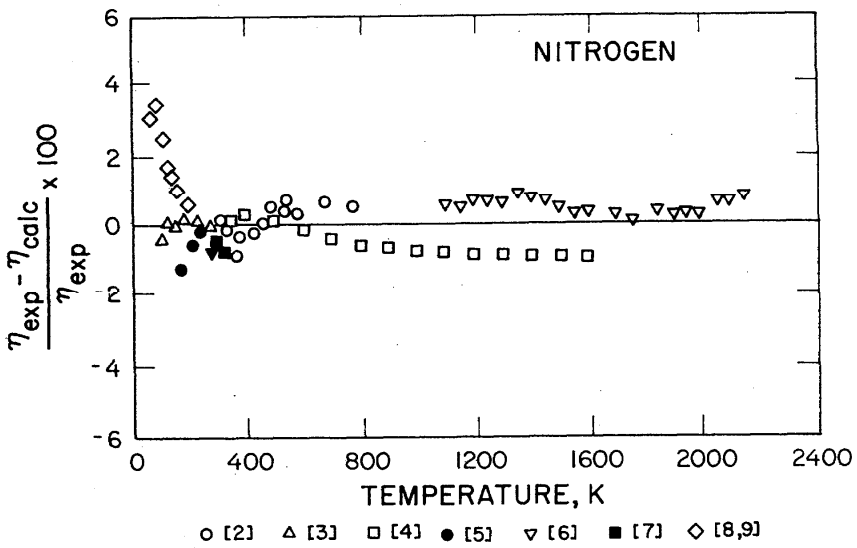

FIGURE 3. Deviations between selected viscosity data and calculated values for nitrogen.

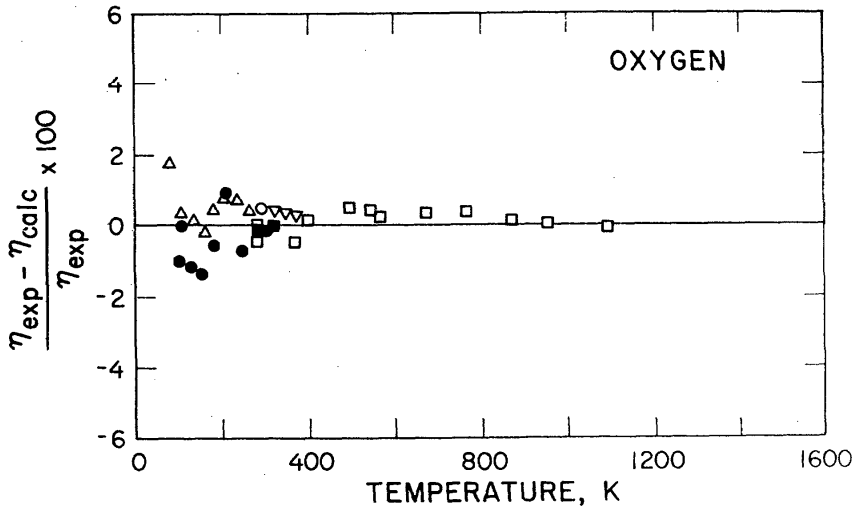

FIGURE 4. Deviations between selected viscosity data and calculated values for oxygen. Key: upside down triangle [7], triangle [8], square [11, 12, 18], filled square [20–22], filled circle [74]. Note, the data of reference [8] have been adjusted at low temperatures. The data of references [11, 12, 18] have been adjusted at high temperatures, see table 2. We have included the recent unpublished data of Haynes [74] in the figure.

Figures 3 and 4 show deviations between experimental viscosity coefficients and the tabulated values. Bearing in mind that much of the viscosity data for oxygen has been adjusted, the curves are satisfactory and indicate a proper correlation has been achieved. One does observe, however, the difference between the data of Guevara [6] and that of Smith [4] for nitrogen. A similar discrepancy was discussed for the rare gases in I but could only be partially resolved. Here, as well, we cannot recommend one set over the other. One also observes that the low temperature nitrogen data of Johnston [8, 9] tends to be high with respect to the correlation and to other equivalent data. We have, however, already remarked (section 2) that these data may be slightly in error.

Figures 5 and 6 illustrate the deviations between tabulated and experimental thermal conductivity coefficients. A first inspection of the figures indicates the correlations are only partially successful because there seems to be systematic differences between theory and

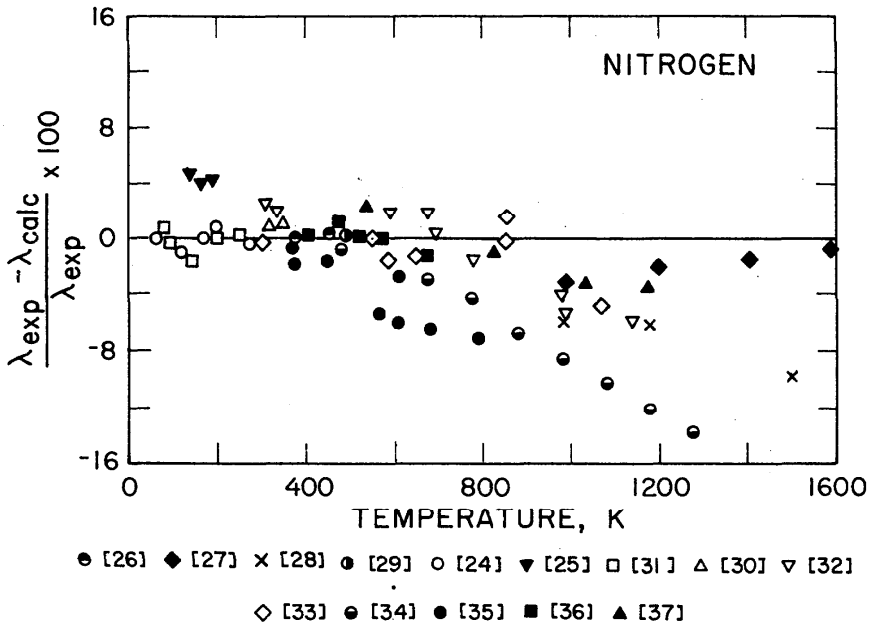

FIGURE 5. Deviations between experimental thermal conductivity coefficients and calculated values for nitrogen.

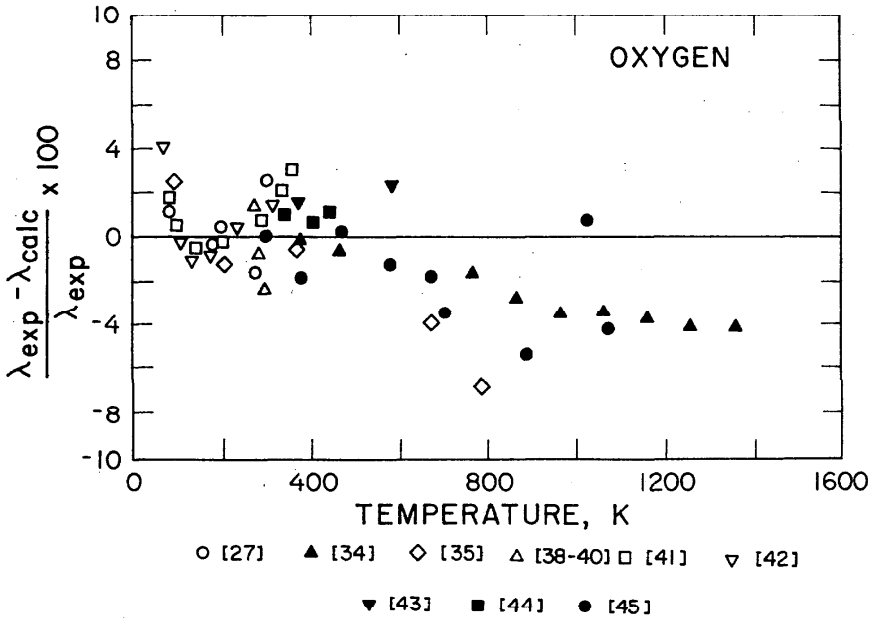

FIGURE 6. Deviations between experimental thermal conductivity coefficients and calculated values for oxygen.

experiment above about 600 K. However, since 1) there are serious difficulties in measuring the thermal conductivity coefficient, 2) the preferred data for nitrogen (references [25], [27], [29], [30], and [37]) are fitted to within four percent, and 3) the approximations made in the kinetic theory formulation become more realistic as the temperature increases—$\Delta\epsilon \ll kT$, Z increases with temperature, and the angularly dependent terms of the potential function have a decreasing effect on the collision integrals as the temperature increases (see the Appendix)—one can suspect that uncertainty in the data are primarily responsible for the large and sometimes systematic deviations in the figures. Clearly, however, the correlation could stand improvement and further reliable data are needed.

5.1. Reliability Assessment

In I, the reliability of the tables for the rare gases was assessed from two viewpoints: an experimental viewpoint in which the correlation was compared to the results from different authors and, especially, to the results from different techniques, and a semi-theoretical viewpoint involving the potential function. It was shown that the model potential suitable for the correlation of the viscosity coefficient could be used to satisfactorily represent the independent properties, the self-diffusion coefficient, the isotopic thermal diffusion factor, and the second virial coefficient.

It is at once apparent that the uncertainty assessment of the tables for the polyatomic gases nitrogen and oxygen cannot be so clear-cut. We will, however, follow the line of arguments adopted for the rare gases.

Experimental

The present correlations are based on viscosity data. For oxygen, the data have been adjusted so that a discussion of experimental errors cannot be too significant. It is encouraging to note, however, that the very recent data of Haynes [74] are within about 1½ percent of the adjusted data at low temperatures. Since we do not think our adjusted values up to 400 K are in error by more than ±2 percent, an uncertainty assessment of ±2 percent to 400 K appears reasonable. Above that temperature the uncertainty assessment is increased to ±4 percent. For nitrogen, the correlation is based on viscosities selected from those selected data sources that have reported data for the rare gases and we have discussed and compared these measurements in I. Practically the same conclusions follow for nitrogen, viz., (a) that selected data from several different procedures—the oscillating disc, and the capillary flow, in particular—and from several different sources, agree to within one percent in the range ~ 100 to 1000 K (see figure 3). Accordingly, we assign an error in the nitrogen viscosity tabulation of ±1 percent in that temperature range. (b) Based on the disagreement between results of Smith and of Guevara at high temperatures, the error is expanded to ±2 percent above 1000 K. (c) Because the data are somewhat suspect at very low temperatures, we also set the error at ±2 percent below 100 K.

The deviation patterns of figures 5 and 6 reflect the uncertainty in the thermal conductivity data. Reliable data are essentially restricted to a room temperature range, and data are sparse above 1500 K for nitrogen and apparently nonexistant for oxygen above this temperature.

Semi-Theoretical

We consider how well the nonspherical potential can represent two properties, the isotopic thermal diffusion factor (α_0) and the second virial coefficient (B) given the parameters of the viscosity correlations. Self-diffusion data for nitrogen and oxygen are not suitable for consideration.

Thermal Diffusion Factor

The expression for the isotopic thermal diffusion factor has been defined for a monatomic gas [1]:

$$\alpha_0 = \alpha_0' [1 + \delta], \tag{22}$$

where

$$\alpha_0' = \frac{15\ (6C^* - 5)\ (2A^* + 5)}{2A^*\ (16A^* - 12B'^* + 55)}, \tag{23}$$

and δ is a correction term written out in I. A^* and C^* have been defined by equations (15) and (14) and B'^* is given by

$$B'^* = \frac{5\langle\Omega^{(1,2)*}\rangle - 4\langle\Omega^{(1,3)*}\rangle}{\langle\Omega^{(1,1)*}\rangle}.$$

Equation (22) is probably too simple for a polyatomic gas [75], but since it is not clear what modifications are required, it is accepted as valid. We have calculated α_0 for nitrogen and oxygen with the angle-averaged collision integrals (see the Appendix) and figures 7 and 8 display the results when compared to experiment [76, 77]. The data are known to be uncertain, so that one cannot attach too much significance to the figures, but it does seem that the experiment is qualitatively represented. In particular, the calculation indicates the sign change of α_0 at low temperatures. Our previous calculations with the spherical m-6-8 potential gave values of α_0 which were always positive for nitrogen [59].

The Second Virial Coefficient

Comparisons between calculated and experimental virial coefficients provide a good test of the potential—and hence of the transport property correlations—because the exact expression for the second virial coefficient of a quadrupolar gas has been published by McQuarrie and Levine [62] (see also [58]), and its

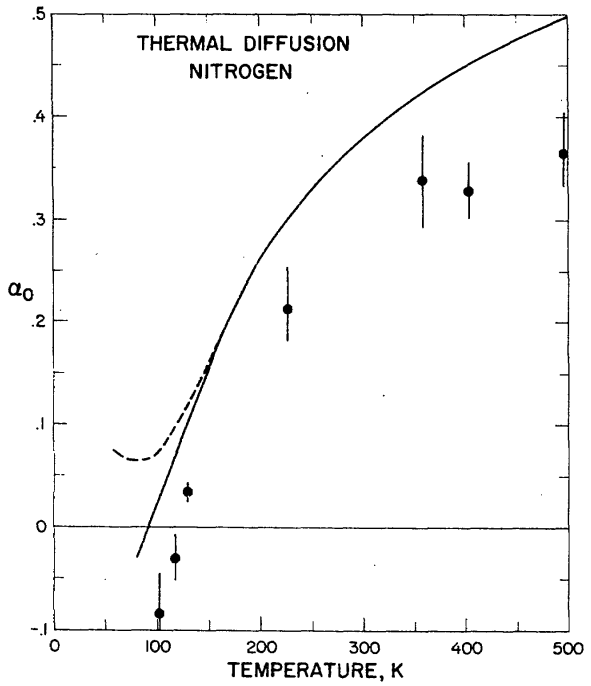

FIGURE 7. Plot of the isotopic thermal diffusion factor for nitrogen calculated from equation (22), data from reference [76] (solid circles).

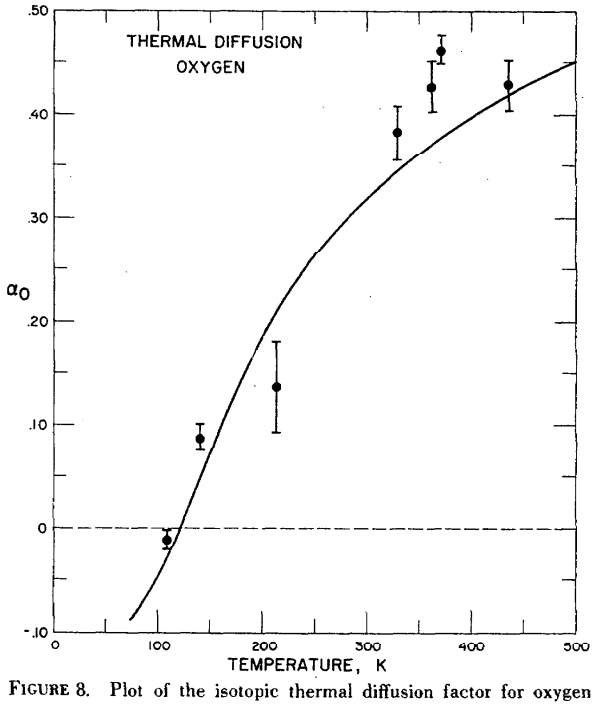

FIGURE 8. Plot of the isotopic thermal diffusion factor for oxygen calculated from equation (22), data from reference [77] (solid circles). Note in figures 7 and 8 that we predict α_0 to change sign.

numerical evaluation is relatively straightforward.

Given the expansion

$$\frac{p}{\rho' N_0 kT} = 1 + B(T)\rho' + \ldots, \tag{24}$$

where p is the pressure, N_0 Avogadro's number, and ρ' the molar density, we have shown [60, 61] that the second virial coefficient for the potential of equation (24) is properly defined by (to terms up to third order in the expansion parameters Θ^{*2} and $\bar{\alpha}^*$):

$$B(T)/b_0 = B^*(T^*)\ [m\text{–}6\text{–}8] - \frac{21}{5}\frac{\Theta^{*4}}{T^{*2}} I_{10} + \frac{216}{245}\frac{\Theta^{*6}}{T^{*3}} I_{15} - \frac{9\bar{\alpha}^*\,\Theta^{*2}}{T^*} I_8 + \frac{108}{25}\frac{\bar{\alpha}^{*2}\,\kappa^2\,\Theta^{*2}}{T^*} I_{11} + \frac{216}{35}\frac{\bar{\alpha}^*\,\kappa\Theta^{*4}}{T^{*2}} I_{13}, \tag{25}$$

where

$$b_0 = 2\pi N_0\,\sigma^3/3, \tag{26}$$

and

$$B^*(T^*)\,[m\text{–}6\text{–}8] = -3\int_0^\infty r^{*2}\,[\exp(-\Phi_s^*/T^*) - 1]\,dr^*, \tag{27}$$

which is the classical reduced virial coefficient of the spherical m–6–8 potential. The quantities I_n are dimensionless integrals given by,

$$I_n = \int_0^\infty r^{*(-n+2)} \exp(-\Phi_s^*/T^*)\,dr^*. \tag{28}$$

Note that the integrals in equations (27) and (28) involve the spherical part of the potential. The integrals were calculated as a function of T^* by means of a Gauss-Legendre integration scheme and the virial coefficients evaluated using the values of $\bar{\alpha}^*$ and Θ^* listed in table 3 with the values of σ and ϵ/k found from the viscosity fits.

Figures 9 and 10 illustrate the deviations between theory and experiment [78]. There are two remarks: (1) The second virial data at low temperatures have an estimated accuracy of about 4 cm^3/mol. (2) We constructed figure 11 which shows two deviation curves and points for nitrogen. The first curve was obtained by calculating the virials from equation (27) with m–6–8 parameters found from a viscosity correlation assuming the collision integrals were angularly independent: $m=12$, $\gamma=2.0$, $\epsilon/k=118.0$ K, $\sigma=3.54\times10^{-10}$ m. The second curve was calculated with the full potential and equation (25), but the m–6–8 parameters were those above [60, 61]. Finally, the points indicate deviations obtained using equation (25) for the virial, but with m–6–8 parameters from the viscosity fit with angle averaged collision integrals (as in figure 9). It is clear that the deviations between experiment and theory are reduced as the calculation procedure becomes more

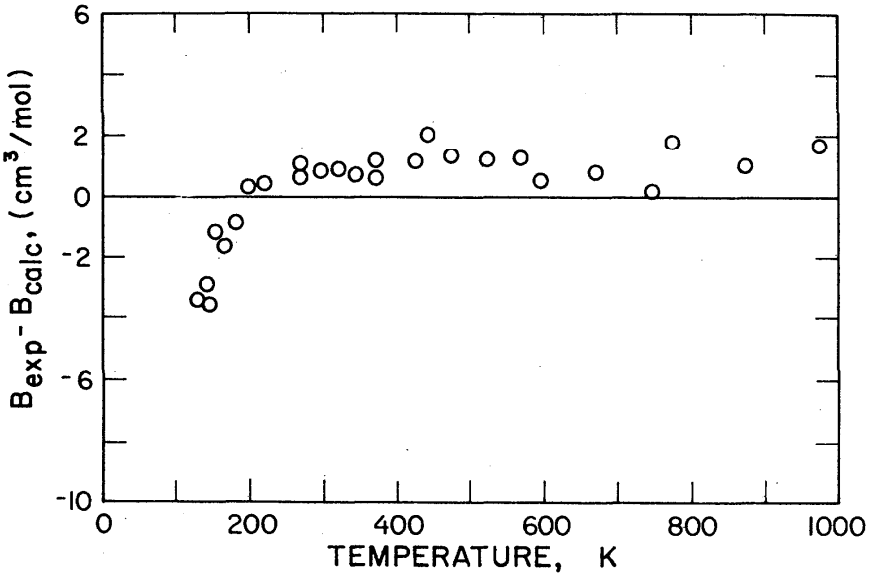

FIGURE 9. Deviation between experimental [78] second virial coefficients and theoretical values calculated from equation (25) for nitrogen.

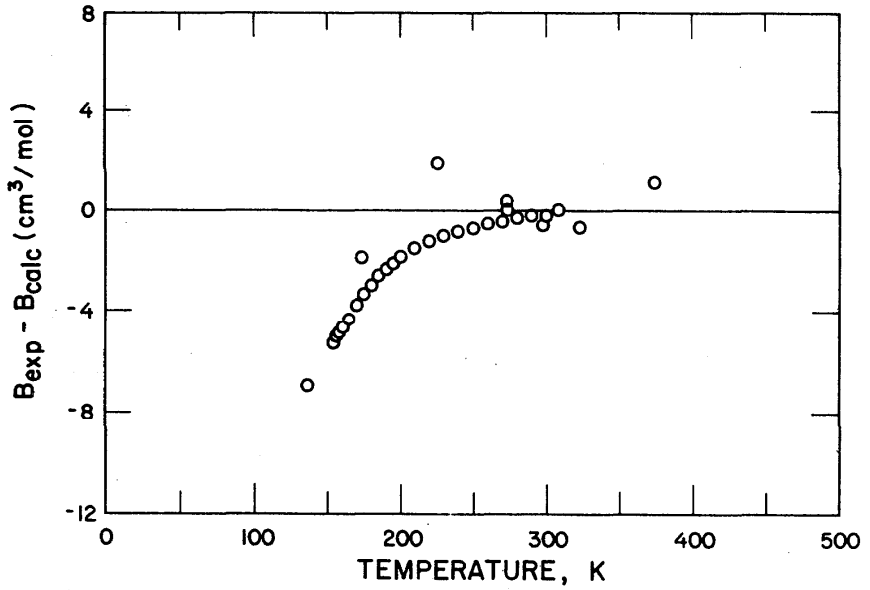

FIGURE 10. Deviation between experimental [78] second virial coefficients and theoretical values calculated from equation (25) for oxygen

complex. The remaining differences between experiment and theory are most probably due to the neglect of anisotropy in the potential. Preliminary calculations have indicated that anisotropy has a small effect on the collision integrals but would increase the calculated second virial by about three percent at the low temperatures (i.e., would improve the representation of experiment). (One can also argue that the assumption that molecules have a fixed relative orientation before collision could be partially responsible for the remaining disagreement in the figure, but this cannot be checked at this time.)

A figure for oxygen, similar to figure 11, was constructed, but the nonspherical contributions to the second virial coefficient are small for this gas, so the differences between the virial calculation procedures

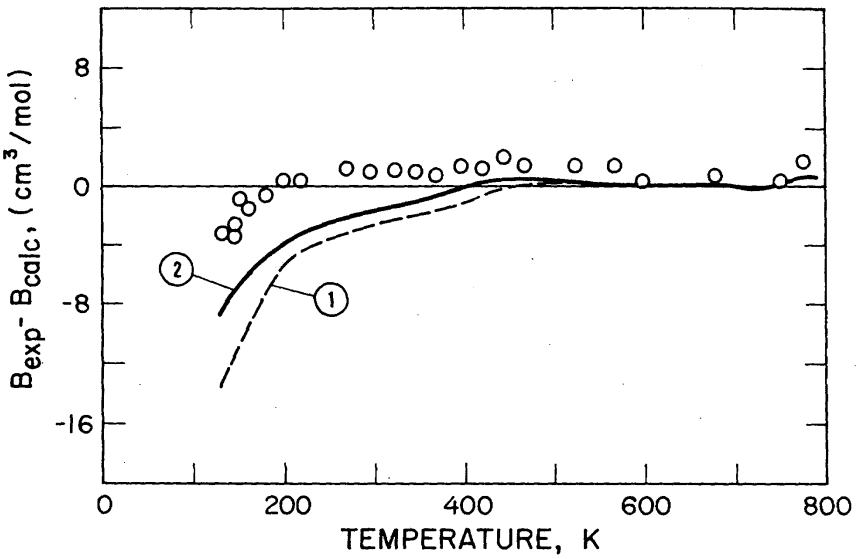

FIGURE 11. Deviations between theory and experiment for the second virial coefficient of nitrogen. The circles are the deviations obtained here using a nonspherical potential and angle averaged collision integrals (as in figure 9). Curve 1 displays the deviations that are obtained assuming the potential is symmetric. Curve 2 gives the deviations observed [60] if a nonspherical potential is used to calculate $B(T)$ but if the parameters are selected for a viscosity correlation with angle *independent* collision integrals.

are not very noticeable. The trend, however, is the same as it is for nitrogen.

Clearly, the application of kinetic theory to nitrogen and oxygen does not allow as definite conclusions as we are able to state for the rare gases [1], but further refinements in the procedure would require very complicated calculations which are not justified by the precision or range of the transport data presently available. Therefore, our conclusions from figures 3–11 are that the calculation procedure adopted is justified, that the representations of the viscosity and thermal conductivity coefficients are mutually consistent for each gas, that the transport properties are consistent with equilibrium properties via the second virial coefficient, and that the error limits reported in the first part of this section are realistic.

5.2. Extrapolation of the Tables

We remarked in I that the extrapolation of the rare gas tables was limited by the potential. At very high or at very low temperatures the m–6–8 model is not sufficiently realistic to allow the tables to be used beyond about 4000 K or below the triple point temperature. The same comment applies in this work only in that extrapolations at high temperatures one must consider that nitrogen and oxygen will dissociate. Further, because (a) the high temperature oxygen data were adjusted, and (b) high temperature thermal conductivity data for both gases are very uncertain, and scarce, we do not recommend that these tables be extrapolated much beyond 2000 K.

6. Conclusion

Tables of the dilute gas viscosity and thermal conductivity coefficients for nitrogen and oxygen have been generated from an m–6–8 potential with nonspherical terms included. The nonspherical contributions did not involve use of extra parameters. On the basis of an analysis of the input data, and from the results observed when the potential found suitable for a correlation of the transport properties was inserted into the statistical mechanical equation for the second virial coefficient, we assess the following uncertainties on the tabulated values: viscosity: oxygen ± 2 percent to 400 K, ± 4 percent for temperatures greater than 400 K; for nitrogen, ± 1 percent in the range 100–1000 K, ± 2 percent for temperatures below 100 K, and above 1000 K. Thermal conductivity, ± 3 percent below 400 K and ± 5 percent above 400 K for both gases.

The paper summarizes the assumptions required in the kinetic theory of dilute polyatomic molecules and points out several gaps in the data coverage for oxygen. It was also noted that most of the data for the thermal conductivity coefficient for both nitrogen and oxygen seem unreliable outside the range of about 150 to 600 K.

We are grateful to the authors of many of the experimental papers discussed for their help in evaluating experimental errors and to W. Michael Haynes in particular for allowing us to use his data prior to publication. Dr. Sengers, of the University of Maryland, and Drs. Guildner and Roder of the National Bureau of

Standards gave many valuable comments on the experimental status of thermal conductivity measurements. We also acknowledge Drs. Mason and Monchick and their co-workers whose papers were indispensable to this research. Much of the computer time required by this study was provided by the National Center for Atmospheric Research which is sponsored by the National Science Foundation.

7. References

[1] Hanley, H. J. M., J. Phys. Chem. Ref. Data **2**, 619 (1973).
[2] Dippo, R., and Kestin, J., "The Viscosity of Seven Gases Up to 500 °C and Its Statistical Interpretation", Brown University Report NSF-GK 13-5 (1967); Kestin, J., Paykoc, E., and Sengers, J. V., Physica **54**, 1 (1971); Kestin, J., Ro, S. T., and Wakeham, W., J. Chem. Phys. **56**, 5837 (1972); Trans. Faraday Soc., **67**, 2308 (1971); Kestin, J., and Whitelaw, Physica **29**, 335 (1963).
[3] Clarke, A. G., and Smith, E. B., J. Chem. Phys. **51**, 4156 (1969).
[4] Dawe, R. A., and Smith, E. B., J. Chem. Phys. **52**, 693 (1970).
[5] Gracki, J. A., Flynn, G. P., and Ross, J., J. Chem. Phys. **51**, 3856 (1969).
[6] Guevara, F. A., McInteer, B. B., and Wageman, W. E., Phys. Fluids **12**, 2493 (1969).
[7] Wobser, R., and Müller, F., Koll-Beih **52**, 165 (1941).
[8] Johnston, H. L., and McCloskey, K. E., J. Phys. Chem. **44**, 1038 (1940).
[9] Johnston, H. L., Mattox, W. R., and Powers, R. W., Nat'l Advisory Comm. Aeronaut. Tech. Note No. 2456 (1951).
[10] Lazarre, F., and Vodar, B., Proc. Conf. Thermodynamic and Transport Properties of Fluids, London, July 1957, Inst. Mech. Engrs., 159 (1958).
[11] Trautz, M., and Melster, A., Ann. Physik **7**, 409 (1930); Trautz, M., and Heberling, R., Ann. Physik **10**, 155 (1931); Trautz, M., and Zimmermann, H., Ann. Physik **22**, 189 (1935).
[12] Raw, C. J. G., and Ellis, C. P., J. Chem. Phys. **28**, 1198 (1958).
[13] Guevara, F. A., McInteer, B. B., Ottesen, D., and Hanley, H. J. M., Los Alamos Scientific Laboratory Report, LA-4643-MS (1970).
[14] Childs, G. E., and Hanley, H. J. M., NBS Tech. Note No. 350 (1966); C. J. G. Raw, Private Communication.
[15] Dawe, R. A., Maitland, G. C., Rigby, M., and Smith, E. B., Trans. Faraday Soc., **66**, 1955 (1970).
[16] Clarke, A. G., and Smith, E. B., J. Chem. Phys. **48**, 3988 (1968).
[17] Johnston, H. L., and Grilly, E. R., J. Phys. Chem. **46**, 948 (1942).
[18] Trautz, M., and Zink, R., Ann. Physik **7**, 427 (1930).
[19] Kestin, J., and Leidenfrost, W., Physica **25**, 1033 (1959).
[20] Andrussow, L., J. Chim. Phys. **52**, 295 (1955).
[21] Von Lierde, J., Verhandel. Koninkl. Vlaam. Acad. Wetenschap. Belg. Kl. Wetenschap. (24) **9**, 7-78 (1947).
[22] Yen. K., Phil. Mag. **38**, 582 (1919).
[23] McLaughlin, E., and Pittman, J. F. T., Phil. Trans. R. Soc. London **A270**, 557 (1971).
[24] Eucken, A., Physik Z. **12**, 1101 (1911).
[25] Ziebland, H., and Burton, J. T. A., Brit. J. Appl. Phys. **9**, 52 (1958).
[26] Le Neindre, B., Int. J. Heat Mass Transfer, **15**, 1 (1971); Le Neindre, B., Thesis; Univ. of Paris (1970).
[27] Faubert, F. M., and Springer, G. S., J. Chem. Phys. **57**, 2333 (1972).
[28] Saxena, S. C., Gupta, G. P., and Saxena, V. K., "Proc. 8th Conf. Thermal Conductivity", C. Y. Ho et al., eds. Plenum Press, New York (1969).
[29] Haarman, J. W., Thesis, Delft, The Netherlands (1969).
[30] Michels, A., and Botzen, A., Physica **19**, 585 (1953).
[31] Golubev, I. F., and Kal'sina, M. V., Gaz. Prom. **9**, 41 (1964). Translation available from SLA translation center, No. LA-TR-65-1.
[32] Vargaftik, N. B., and Zimina, N. Kh., High Temp. **2**, 782 (1964).
[33] Westenberg, A. A., and deHaas, N., Phys. Fluids **5**, 266 (1962).
[34] Geier, H., and Schäfer, K., Allgem, Warmetech. **10**, 70 (1961).
[35] Franck, E. U., Chem. Eng. Tech. **25**, 238 (1953); Z. Electrochem **55**, 636 (1951).
[36] Vines, R. G., Mass. Inst. of Tech., Tech. Report MIT-20-P (Sept. 1958), DDC AD 205 694.
[37] Nuttall, R. L., and Ginnings, D. C., J. Res. Nat. Bur. Stand. (U.S.), **58** No. 5, 271-278 (May 1957).
[38] Gregory, H., and Marshall, S., Proc. Roy. Soc. (London) **A118**, 594 (1928).
[39] Kannuluik, W. G., and Martin, L. H., Proc. Roy. Soc. (London) **A144**, 496 (1934).
[40] Nothdurft, W., Ann. Physik **28**, 137 (1937).
[41] Johnston, H. L., and Grilly, E. R., J. Chem. Phys. **14**, 233 (1946).
[42] Tsederberg, N. V., and Timrot, D. L., Soviet Phys. Tech. Phys. **1**, 1791 (1956).
[43] Cheung, H., Thermal Conductivity and Viscosity of Gas Mixtures, Calif. Univ., Lawrence Radiation Lab., Berkeley, Report No. UCRL-8230 (April 1958).
[44] Pereira, A. N. G., and Raw, C. J. G., Phys. Fluids **6**, 1091 (1963).
[45] Westenberg, A. A., and deHaas, N., Phys. Fluids **6**, 617 (1963).
[46] Ho, C. Y., Powell, R. W., and Liley, P. E., J. Phys. Chem. Ref. Data **1**, 279 (1972).
[47] Maitland, G. C., and Smith, E. B., J. Chem. Eng. Data **17**, 150 (1972).
[48] Vasserman, A. A., Kazavchinskii, Y. Z., and Rabinovich, V. A., Thermophysical Properties of Air and Air Components. (Israel Program for Scientific Translations, Jerusalem, 1971). Available from the National Bureau of Standards, Washington, D.C. 20234.
[49] Wang Chang, C. S., and Uhlenbeck, G. E., Univ. of Mich. Eng. Res. Report No. CM-681 (1958).
[50] Taxman, N., Phys. Rev. **110**, 1235 (1958).
[51] Wang Chang, C. S., Uhlenbeck, G. E., and de Boer, J., *Studies in Statistical Mechanics*, Vol. 2, J. de Boer and G. E. Uhlenbeck, eds., (John Wiley, New York, 1964) pp. 241-268.
[52] Mason, E. A., Proc. 4th Sym. on Thermophy. Prop. ASME, New York (1968). p. 21.
[53] Monchick, L., and Mason, E. A., J. Chem. Phys. **35**, 1676 (1961).
[54] Monchick, L., Pereira, A. N. G., and Mason, E. A., J. Chem. Phys. **42**, 3241 (1965).
[55] Mason, E. A., and Monchick, L., J. Chem. Phys. **36**, 1622 (1962).
[56] Sandler, S. I., Phys. Fluids, **11**, 2549 (1968).
[57] Mason, E. A., Vanderslice, J. T., and Yos, J. M., Phys. Fluids **2**, 688 (1959).
[58] Mason, E. A., and Spurling, T. H., *The Virial Equation of State*, Pergamon Press, New York (1969), p. 204.
[59] Hanley, H. J. M., and Klein, M., Nat. Bur. Stand. Tech. Note No. 628 (1972).
[60] Ely, J. F., and Hanley, H. J. M., Mol. Phys. **24**, 684 (1972).
[61] Ely, J. F., Hanley, H. J. M., and Straty, G. C., J. Chem. Phys. **59**, 842 (1973).
[62] McQuarrie, D. A., and Levine, H. B., Physica, **31**, 749 (1965).
[63] Isihara, A., and Hanks, R. V., J. Chem. Phys. **36**, 433 (1962).
[64] Oudemans, G. J., Ph. D Thesis, Univ. of Amsterdam (1967).
[65] Younglove, B., J. Res. Nat. Bur. Stand. **A76**, 37 (1972).
[66] Buckingham, A. D., Disch, R. L., and Dunmur, D. A., J. Am. Chem. Soc. **90**, 3104 (1968).
[67] Bridge, N. J., and Buckingham, A. D., Proc. R. Soc. (London) **A295**, 334 (1966).
[68] Prangsma, G. J., Alberga, A. H., and Beenakker, J. J. M., Physica, **64**, 278 (1973).
[69] Ganzi, G., and Sandler, S. I., J. Chem. Phys. **55**, 132 (1971).
[70] Annis, B. K., and Malinauskas, A. P., J. Chem. Phys. **54**, 4763 (1971).

[71] Carnevale, E. H., Carey, C., and Larson, G., J. Chem. Phys. **47**, 2829 (1967).
[72] Baehr, H. D., Hartmann, H., Pohl, H. C., and Schomäcker, H., *Thermodynamische Eigenschaften der Gase und Flussigkeiten*, Vol. 2 (Springer-Verlag, Berlin 1968).
[73] Woolley, H. W., J. Res. Nat. Bur. Stand. (U.S.), **40**, 163 (1948).
[74] Haynes, W. M., Private Communication. Unpublished results available from NBS, Boulder, Colorado.
[75] Monchick, L., Sandler, S. I., and Mason, E. A., J. Chem. Phys. **49**, 1178 (1968).
[76] Raman, S., Mathur, B. P., Howard, A. J., Champlin, J. W., and Watson, W. W., J. Chem. Phys. **49**, 4877 (1968).
[77] Mathur, B. P., and Watson, W. W., J. Chem. Phys. **51**, 2210 (1969).
[78] Experimental second virial coefficients have been carefully evaluated and listed in: Levelt Sengers, J. M. H., Klein, M., and Gallagher, J. S., AIP Handbook, McGraw-Hill, New York (1972), ed. Gray, D. E.
[79] O'Hara, H., and Smith, Francis, J., J. Comp. Phys. **5**, 328 (1970). Also see Smith, F. J., Physica **30**, 497 (1964) and Smith, F. J., and Munn, R. J., Chem. Phys. **41**, 3560 (1964).
[80] Smith, Francis J., Munn, R. J., and Mason, E. A., J. Chem. Phys. **46**, 317 (1967).

TABLE 1. References for the dilute gas viscosity and thermal conductivity correlations

Gas	Viscosity references	Thermal conductivity references
N_2	[2–10]	[24–37]
O_2	Adjusted data, table 2 [7], [19–22], see also [74].	[24, 35, 38–45]

TABLE 2. Adjusted experimental viscosities for oxygen

Temperature K	Viscosity 10^3 g/cm s	Temperature K	Viscosity 10^3 g/cm s
90.3	0.0679	500.1	0.305
118.8	.0890	550.1	.327
131.3	.0979	556.1	.328
144.9	.108	675.1	.377
158.5	.117	769.1	.411
172.6	.128	881.1	.450
184.6	.137	963.1	.477
400.8	.258	1102.1	.521

TABLE 3. Potential parameters

Gas	m	γ	$\sigma(10^{-10}$ m)	ϵ/k, K	$10^{24}\alpha$, cm^3	Θ, 10^{26}, esu	κ
N_2	12	0.5	3.613	102.0	1.737[64]	1.40[66]	0.134[67]
O_2	10	1.0	3.463	109.5	1.568[65]	.4 [66]	.213[67]

TABLE 4. Viscosity and thermal conductivity coefficients of nitrogen. Units: viscosity, 10^3 g/cm · s, thermal conductivity, 10^3 W/cm · K.

TEMPERATURE K	VISCOSITY G/CM·S $10^3\eta$	THERMAL CONDUCTIVITY W/CM·K $10^3\lambda$	TEMPERATURE K	VISCOSITY G/CM·S $10^3\eta$	THERMAL CONDUCTIVITY W/CM·K $10^3\lambda$
80	0.0540	0.0750	170	0.1118	0.1579
85	0.0573	0.0798	175	0.1147	0.1621
90	0.0607	0.0846	180	0.1176	0.1664
95	0.0641	0.0894	185	0.1205	0.1705
100	0.0675	0.0942	190	0.1233	0.1747
			195	0.1262	0.1788
105	0.0708	0.0989	200	0.1290	0.1829
110	0.0741	0.1037			
115	0.0774	0.1084	205	0.1317	0.1869
120	0.0807	0.1131	210	0.1344	0.1909
125	0.0840	0.1178	215	0.1371	0.1948
130	0.0872	0.1223	220	0.1398	0.1988
135	0.0904	0.1269	225	0.1425	0.2027
140	0.0935	0.1315	230	0.1451	0.2065
145	0.0967	0.1360	235	0.1477	0.2103
150	0.0997	0.1404	240	0.1502	0.2141
			245	0.1528	0.2179
155	0.1028	0.1449	250	0.1553	0.2216
160	0.1058	0.1493			
165	0.1088	0.1536	255	0.1578	0.2253

TABLE 4. Viscosity and thermal conductivity coefficients of nitrogen. Units: viscosity, 10^3 g/cm·s, thermal conductivity, 10^3 W/cm·K. – Continued

TEMPERATURE K	VISCOSITY G/CM-S $10^3\eta$	THERMAL CONDUCTIVITY W/CM-K $10^3\lambda$	TEMPERATURE K	VISCOSITY G/CM-S $10^3\eta$	THERMAL CONDUCTIVITY W/CM-K $10^3\lambda$
260	0.1603	0.2290	580	0.2887	0.4324
265	0.1628	0.2327	590	0.2921	0.4384
270	0.1652	0.2363	600	0.2955	0.4444
275	0.1676	0.2399			
280	0.1700	0.2434	610	0.2988	0.4505
285	0.1724	0.2470	620	0.3021	0.4563
290	0.1747	0.2505	630	0.3054	0.4624
295	0.1771	0.2539	640	0.3087	0.4683
300	0.1794	0.2574	650	0.3119	0.4743
			660	0.3151	0.4803
305	0.1817	0.2609	670	0.3183	0.4863
310	0.1840	0.2643	680	0.3215	0.4922
315	0.1862	0.2677	690	0.3247	0.4982
320	0.1885	0.2711	700	0.3279	0.5042
325	0.1907	0.2744			
330	0.1929	0.2777	710	0.3310	0.5102
335	0.1951	0.2811	720	0.3341	0.5160
340	0.1973	0.2844	730	0.3372	0.5220
345	0.1995	0.2877	740	0.3403	0.5280
350	0.2016	0.2909	750	0.3433	0.5339
			760	0.3463	0.5398
355	0.2038	0.2942	770	0.3494	0.5457
360	0.2059	0.2975	780	0.3524	0.5517
365	0.2080	0.3007	790	0.3554	0.5576
370	0.2101	0.3039	800	0.3584	0.5635
375	0.2122	0.3071			
380	0.2142	0.3103	810	0.3613	0.5694
385	0.2163	0.3135	820	0.3643	0.5752
390	0.2183	0.3166	830	0.3671	0.5810
395	0.2204	0.3198	840	0.3701	0.5870
400	0.2224	0.3229	850	0.3730	0.5924
			860	0.3759	0.5981
405	0.2244	0.3261	870	0.3788	0.6038
410	0.2264	0.3291	880	0.3817	0.6095
415	0.2284	0.3323	890	0.3845	0.6151
420	0.2303	0.3353	900	0.3874	0.6207
425	0.2322	0.3384			
430	0.2342	0.3415	910	0.3902	0.6263
435	0.2361	0.3445	920	0.3930	0.6319
440	0.2380	0.3476	930	0.3957	0.6375
445	0.2399	0.3506	940	0.3986	0.6431
450	0.2419	0.3537	950	0.4013	0.6487
			960	0.4041	0.6543
455	0.2438	0.3568	970	0.4069	0.6598
460	0.2457	0.3598	980	0.4096	0.6654
465	0.2475	0.3629	990	0.4123	0.6709
470	0.2494	0.3660	1000	0.4150	0.6764
475	0.2513	0.3690			
480	0.2532	0.3721	1010	0.4177	0.6818
485	0.2550	0.3752	1020	0.4204	0.6872
490	0.2569	0.3782	1030	0.4230	0.6924
495	0.2587	0.3812	1040	0.4255	0.6977
500	0.2606	0.3843	1050	0.4285	0.7037
			1060	0.4312	0.7092
510	0.2642	0.3904	1070	0.4339	0.7146
520	0.2678	0.3964	1080	0.4365	0.7200
530	0.2713	0.4024	1090	0.4392	0.7254
540	0.2748	0.4083	1100	0.4418	0.7308
550	0.2783	0.4143			
560	0.2818	0.4204	1110	0.4444	0.7361
570	0.2852	0.4264	1120	0.4469	0.7412

TABLE 4. Viscosity and thermal conductivity coefficients of nitrogen. Units: viscosity, 10^3 g/cm · s, thermal conductivity, 10^3 W/cm · K. — Continued

TEMPERATURE K	VISCOSITY G/CM-S $10^3\eta$	THERMAL CONDUCTIVITY W/CM-K $10^3\lambda$	TEMPERATURE K	VISCOSITY G/CM-S $10^3\eta$	THERMAL CONDUCTIVITY W/CM-K $10^3\lambda$
1130	0.4495	0.7465	1570	0.5562	0.9655
1140	0.4521	0.7520	1580	0.5585	0.9703
1150	0.4547	0.7573	1590	0.5608	0.9750
1160	0.4573	0.7625	1600	0.5631	0.9797
1170	0.4599	0.7678			
1180	0.4624	0.7731	1610	0.5654	0.9843
1190	0.4650	0.7783	1620	0.5677	0.9890
1200	0.4675	0.7835	1630	0.5700	0.9936
			1640	0.5723	0.9982
1210	0.4700	0.7886	1650	0.5745	1.0029
1220	0.4726	0.7938	1660	0.5768	1.0075
1230	0.4751	0.7989	1670	0.5791	1.0121
1240	0.4776	0.8042	1680	0.5813	1.0168
1250	0.4801	0.8093	1690	0.5836	1.0213
1260	0.4826	0.8144	1700	0.5858	1.0259
1270	0.4851	0.8195			
1280	0.4875	0.8246	1710	0.5880	1.0304
1290	0.4900	0.8297	1720	0.5903	1.0349
1300	0.4924	0.8347	1730	0.5925	1.0395
			1740	0.5947	1.0440
1310	0.4949	0.8397	1750	0.5969	1.0484
1320	0.4973	0.8447	1760	0.5991	1.0529
1330	0.4998	0.8497	1770	0.6013	1.0570
1340	0.5022	0.8546	1780	0.6035	1.0615
1350	0.5046	0.8597	1790	0.6057	1.0660
1360	0.5070	0.8647	1800	0.6079	1.0704
1370	0.5094	0.8696			
1380	0.5118	0.8745	1810	0.6101	1.0748
1390	0.5142	0.8794	1820	0.6122	1.0796
1400	0.5166	0.8843	1830	0.6144	1.0840
			1840	0.6166	1.0883
1410	0.5190	0.8892	1850	0.6187	1.0927
1420	0.5213	0.8940	1860	0.6208	1.0970
1430	0.5236	0.8988	1870	0.6230	1.1014
1440	0.5264	0.9040	1880	0.6251	1.1057
1450	0.5287	0.9087	1890	0.6272	1.1100
1460	0.5310	0.9139	1900	0.6294	1.1143
1470	0.5333	0.9186			
1480	0.5356	0.9233	1910	0.6315	1.1186
1490	0.5379	0.9280	1920	0.6336	1.1228
1500	0.5401	0.9327	1930	0.6357	1.1271
			1940	0.6378	1.1313
1510	0.5424	0.9373	1950	0.6398	1.1355
1520	0.5446	0.9419	1960	0.6419	1.1397
1530	0.5469	0.9464	1970	0.6440	1.1439
1540	0.5491	0.9510	1980	0.6460	1.1481
1550	0.5513	0.9555	1990	0.6481	1.1523
1560	0.5535	0.9601	2000	0.6501	1.1564

TABLE 5. Viscosity and thermal conductivity coefficients of oxygen. Units: Viscosity, 10^3 g/cm · s, thermal conductivity, 10^3 W/cm · K.

TEMPERATURE K	VISCOSITY G/CM-S $10^3\eta$	THERMAL CONDUCTIVITY W/CM-K $10^3\lambda$	TEMPERATURE K	VISCOSITY G/CM-S $10^3\eta$	THERMAL CONDUCTIVITY W/CM-K $10^3\lambda$
80	0.0586	0.0696	100	0.0742	0.0897
85	0.0625	0.0746			
90	0.0664	0.0797	105	0.0780	0.0947
95	0.0703	0.0847	110	0.0819	0.0997

TABLE 5. Viscosity and thermal conductivity coefficients of oxygen. Units: Viscosity, 10^3 g/cm·s, thermal conductivity, 10^3 W/cm·K.—Continued

TEMPERATURE K	VISCOSITY G/CM-S $10^3\eta$	THERMAL CONDUCTIVITY W/CM-K $10^3\lambda$	TEMPERATURE K	VISCOSITY G/CM-S $10^3\eta$	THERMAL CONDUCTIVITY W/CM-K $10^3\lambda$
115	0.0857	0.1046	385	0.2502	0.3255
120	0.0895	0.1096	390	0.2527	0.3291
125	0.0933	0.1144	395	0.2551	0.3328
130	0.0971	0.1193	400	0.2575	0.3365
135	0.1008	0.1241			
140	0.1045	0.1289	405	0.2599	0.3402
145	0.1081	0.1336	410	0.2623	0.3439
150	0.1118	0.1384	415	0.2647	0.3476
			420	0.2670	0.3512
155	0.1154	0.1430	425	0.2694	0.3549
160	0.1190	0.1476	430	0.2717	0.3586
165	0.1225	0.1522	435	0.2741	0.3622
170	0.1260	0.1568	440	0.2763	0.3658
175	0.1295	0.1613	445	0.2786	0.3695
180	0.1329	0.1657	450	0.2809	0.3731
185	0.1362	0.1701			
190	0.1396	0.1745	455	0.2831	0.3767
195	0.1429	0.1788	460	0.2854	0.3803
200	0.1462	0.1831	465	0.2876	0.3839
			470	0.2898	0.3876
205	0.1495	0.1874	475	0.2921	0.3912
210	0.1527	0.1916	480	0.2943	0.3948
215	0.1559	0.1958	485	0.2965	0.3984
220	0.1591	0.2000	490	0.2987	0.4020
225	0.1623	0.2041	495	0.3009	0.4056
230	0.1654	0.2082	500	0.3031	0.4092
235	0.1685	0.2122			
240	0.1715	0.2163	510	0.3074	0.4164
245	0.1745	0.2202	520	0.3118	0.4236
250	0.1775	0.2242	530	0.3161	0.4308
			540	0.3203	0.4380
255	0.1805	0.2282	550	0.3245	0.4450
260	0.1835	0.2322	560	0.3287	0.4521
265	0.1864	0.2361	570	0.3328	0.4591
270	0.1893	0.2400	580	0.3369	0.4662
275	0.1921	0.2439	590	0.3409	0.4732
280	0.1950	0.2477	600	0.3450	0.4802
285	0.1978	0.2515			
290	0.2006	0.2553	610	0.3490	0.4872
295	0.2034	0.2591	620	0.3530	0.4942
300	0.2062	0.2628	630	0.3570	0.5012
			640	0.3609	0.5082
305	0.2089	0.2666	650	0.3648	0.5151
310	0.2116	0.2704	660	0.3687	0.5219
315	0.2143	0.2741	670	0.3726	0.5289
320	0.2170	0.2778	680	0.3764	0.5357
325	0.2197	0.2814	690	0.3802	0.5425
330	0.2223	0.2851	700	0.3839	0.5493
335	0.2249	0.2888			
340	0.2275	0.2925	710	0.3877	0.5560
345	0.2301	0.2961	720	0.3915	0.5627
350	0.2327	0.2998	730	0.3952	0.5695
			740	0.3989	0.5762
355	0.2352	0.3035	750	0.4026	0.5828
360	0.2378	0.3072	760	0.4063	0.5894
365	0.2403	0.3109	770	0.4099	0.5959
370	0.2428	0.3145	780	0.4134	0.6024
375	0.2453	0.3181	790	0.4171	0.6089
380	0.2478	0.3218	800	0.4207	0.6154

TABLE 5. Viscosity and thermal conductivity coefficients of oxygen. Units: Viscosity, 10^3 g/cm·s, thermal conductivity, 10^3 W/cm·K.—Continued

TEMPERATURE K	VISCOSITY G/CM·S $10^3\eta$	THERMAL CONDUCTIVITY W/CM·K $10^3\lambda$	TEMPERATURE K	VISCOSITY G/CM·S $10^3\eta$	THERMAL CONDUCTIVIT W/CM·K $10^3\lambda$
810	0.4243	0.6218	1360	0.6007	0.9395
820	0.4278	0.6282	1370	0.6036	0.9448
830	0.4313	0.6346	1380	0.6065	0.9501
840	0.4349	0.6410	1390	0.6094	0.9554
850	0.4384	0.6473	1400	0.6123	0.9606
860	0.4419	0.6536			
870	0.4453	0.6599	1410	0.6152	0.9659
880	0.4488	0.6662	1420	0.6181	0.9711
890	0.4521	0.6723	1430	0.6210	0.9763
900	0.4557	0.6786	1440	0.6239	0.9815
			1450	0.6267	0.9867
910	0.4591	0.6852	1460	0.6296	0.9919
920	0.4625	0.6913	1470	0.6324	0.9971
930	0.4659	0.6973	1480	0.6353	1.0023
940	0.4692	0.7034	1490	0.6381	1.0074
950	0.4726	0.7094	1500	0.6409	1.0126
960	0.4759	0.7154			
970	0.4792	0.7213	1510	0.6437	1.0177
980	0.4825	0.7272	1520	0.6465	1.0228
990	0.4858	0.7331	1530	0.6493	1.0279
1000	0.4890	0.7390	1540	0.6521	1.0330
			1550	0.6549	1.0381
1010	0.4924	0.7449	1560	0.6581	1.0436
1020	0.4957	0.7507	1570	0.6609	1.0490
1030	0.4989	0.7565	1580	0.6636	1.0540
1040	0.5022	0.7623	1590	0.6663	1.0590
1050	0.5054	0.7683	1600	0.6690	1.0640
1060	0.5086	0.7740			
1070	0.5118	0.7798	1610	0.6717	1.0689
1080	0.5150	0.7855	1620	0.6744	1.0739
1090	0.5181	0.7912	1630	0.6770	1.0788
1100	0.5212	0.7967	1640	0.6797	1.0837
			1650	0.6823	1.0886
1110	0.5242	0.8021	1660	0.6850	1.0935
1120	0.5272	0.8078	1670	0.6876	1.0984
1130	0.5308	0.8138	1680	0.6907	1.1041
1140	0.5340	0.8195	1690	0.6935	1.1092
1150	0.5371	0.8252	1700	0.6962	1.1143
1160	0.5403	0.8309			
1170	0.5434	0.8365	1710	0.6990	1.1194
1180	0.5465	0.8420	1720	0.7017	1.1245
1190	0.5495	0.8474	1730	0.7044	1.1296
1200	0.5526	0.8529	1740	0.7072	1.1347
			1750	0.7099	1.1397
1210	0.5556	0.8584	1760	0.7126	1.1448
1220	0.5587	0.8639	1770	0.7153	1.1498
1230	0.5618	0.8694	1780	0.7180	1.1549
1240	0.5648	0.8748	1790	0.7207	1.1600
1250	0.5678	0.8803	1800	0.7234	1.1650
1260	0.5709	0.8858			
1270	0.5739	0.8913	1810	0.7261	1.1700
1280	0.5769	0.8967	1820	0.7288	1.1750
1290	0.5799	0.9021	1830	0.7314	1.1796
1300	0.5829	0.9075	1840	0.7341	1.1846
			1850	0.7367	1.1896
1310	0.5859	0.9128	1860	0.7394	1.1946
1320	0.5889	0.9182	1870	0.7420	1.1996
1330	0.5918	0.9235	1880	0.7447	1.2046
1340	0.5948	0.9288	1890	0.7473	1.2095
1350	0.5977	0.9341	1900	0.7499	1.2145

TABLE 5. Viscosity and thermal conductivity coefficients of oxygen. Units: Viscosity, 10^3 g/cm · s, thermal conductivity, 10^3 W/cm · K.—Con.

TEMPERATURE K	VISCOSITY G/CM-S $10^3\eta$	THERMAL CONDUCTIVITY W/CM-K $10^3\lambda$	TEMPERATURE K	VISCOSITY G/CM-S $10^3\eta$	THERMAL CONDUCTIVITY W/CM-K $10^3\lambda$
1910	0.7525	1.2194	1960	0.7655	1.2441
1920	0.7552	1.2244	1970	0.7681	1.2491
1930	0.7578	1.2293	1980	0.7707	1.2540
1940	0.7604	1.2343	1990	0.7732	1.2589
1950	0.7629	1.2392	2000	0.7758	1.2638

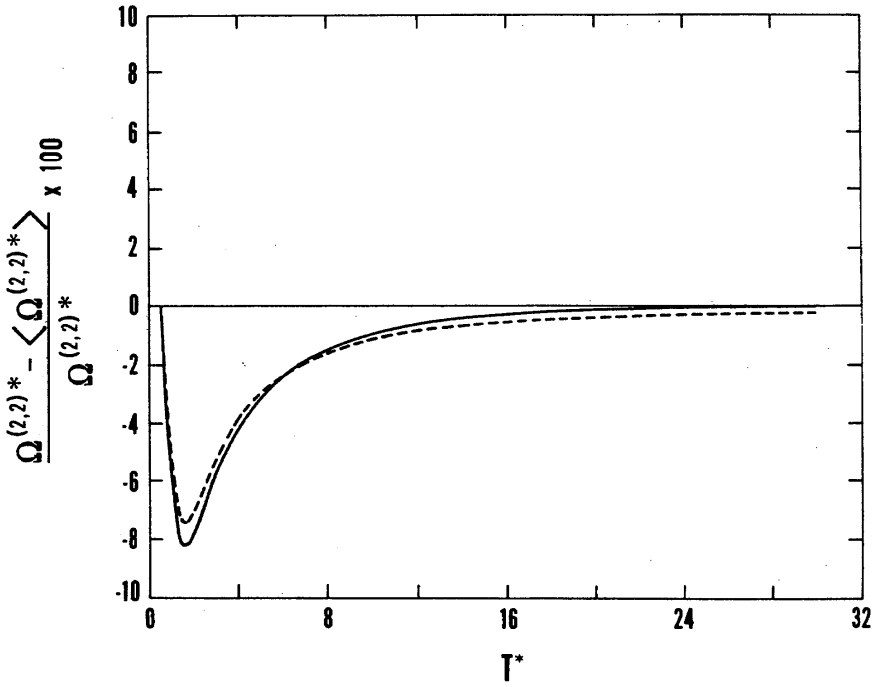

FIGURE 12. Deviations between angle averaged and angle independent collision integrals.

Appendix

The evaluation of the angle averaged collision integrals is a straight forward task under the assumptions of section 3.1. Briefly, if it is assumed that the relative orientation of the colliding pair of molecules doesn't change during the collision and that there are no inelastic effects, we must evaluate the triple integral:

$$\langle\Omega^{(l,s)*}(T^*)\rangle \equiv \frac{1}{8\pi}\int_0^{\pi} d\theta_1 \sin\theta \int_0^{\pi} d\theta_2$$

$$\sin\theta_2 \int_0^{2\pi} d\phi\, \Omega^{(l,s)*}(T^*\theta_1, \theta_2, \phi),$$

where θ_1, θ_2, and ϕ are the angles appearing in equations (20) and (21). We first write this triple integral as a numerical quadrature, viz.

$$\langle\Omega^{(l,s)*}(T^*)\rangle \simeq \frac{1}{8\pi}\sum_{i=0}^{N_i}\sum_{j=0}^{N_k}\sum_{l=0}^{N_l} W_{1,i}\, W_{2,j}\, W_{3,k}\, \Omega^{(l,s)*}(T^*, \omega_{ijk}),$$

where the $W_{\alpha,\beta}$'s are the appropriate weight factors for the quadrature and ω_{ijk} denotes the set of three angles describing the relative orientation, $(\theta_{1i}, \theta_{2j}, \phi_k)$. We next evaluate the collision integrals at a fixed orientation $\Omega^{(l,s*)}(T^*, \omega_{ijk})$, by the method of O'Hara and Smith [79] [the same method as was used for the spherical m–6–8 collision integrals in I] with the appropriate modifications for non-sphericity in the intermolecular potential.

This method of evaluating the angle-averaged collision integrals differs slightly from that used by Smith, et al., [80] who (1) employed an interpolation technique to

obtain the $\Omega^{(l,s)*}$ (T^*, ω_{ijk}) from a table rather than a direct calculation and (2) incorporated a slightly different (we believe less accurate) version of the O'Hara and Smith program.

Tables of collision integrals used in this research are given as tables 6 and 7. The accuracy of our calculations was checked by means of comparison with previous results [80] and by examining the finite differences obtained from the final $\langle\Omega^{(l,s)*}(T^*)\rangle$ vs T^* tables. Overall, the accuracy of these collision is believed to be no worse than 0.1 percent which should be more than adequate for most applications.

As a matter of interest, we include figure 12 which gives a percentage difference plot between angularly averaged and equivalent angular independent collision integrals versus temperature. For comparison, Φ_s was selected to be the Lennard-Jones (12–6) potential. The solid curve shows the percentage difference found by using equation (19) with $\alpha^*=0$ and $\Theta^*=1$, and the dashed curve shows the corresponding differences for $\alpha^*=0.05$ and $\Theta^*=1$. Since most reduced quadrupole moments are approximately 0.3−0.6, these results can be considered to be extreme cases. It is observed, however, that the primary effect of the nonspherical terms is to increase the collision integrals at a given T^* with the maximum effect being around $T^*=2$ and decreasing rapidly with increasing temperature. The addition of an induced-dipole term in the potential makes a small but significant contribution. This term has not been considered previously.

TABLE 6. N_2 collision integrals

T^*	$\langle\Omega^{(1,1)*}\rangle$	$\langle\Omega^{(1,2)*}\rangle$	$\langle\Omega^{(2,2)*}\rangle$	$\langle\Omega^{(1,3)*}\rangle$	$\langle\Omega^{(2,3)*}\rangle$	$\langle\Omega^{(3,3)*}\rangle$
.600	1.85216327	1.54068268	2.05119289	1.34147244	1.80121953	1.67216995
.700	1.71330460	1.42480938	1.90027894	1.24824495	1.66176124	1.54903814
.800	1.60211757	1.33573792	1.77648587	1.17868594	1.55186904	1.45224720
.900	1.51158561	1.26565559	1.67403857	1.12505651	1.46418755	1.37462658
1.000	1.43678465	1.20935675	1.58862778	1.08258502	1.39315912	1.31141026
1.200	1.32101895	1.12489602	1.45559724	1.01952530	1.28632300	1.21522633
1.400	1.23612749	1.06481219	1.35797730	.97480357	1.21060229	1.14608479
1.600	1.17150425	1.01982115	1.28409995	.94115132	1.15450468	1.09420377
1.800	1.12072698	.98482630	1.22651298	.91468092	1.11139090	1.05389492
2.000	1.07984472	.95669350	1.18048580	.89313838	1.07717628	1.02166824
2.200	1.04614715	.93346781	1.14298111	.87511811	1.04931196	.99525607
2.400	1.01786684	.91389353	1.11181087	.85971073	1.02612579	.97315045
2.600	.99379487	.89710234	1.08546283	.84630605	1.00646469	.95432448
2.800	.97301280	.88247382	1.06287905	.83447626	.98951827	.93805167
3.000	.95482717	.86955920	1.04329328	.82390985	.97471069	.92380054
3.200	.93875359	.85803325	1.02612544	.81437643	.96161862	.91117820
3.400	.92442599	.84765223	1.01092247	.80570037	.94992517	.89988721
3.600	.91155889	.83822832	.99733498	.79774627	.93938696	.88969908
3.800	.89991910	.82961209	.98509682	.79040776	.92981501	.88043649
4.000	.88931834	.82168452	.97399672	.78359930	.92106022	.87195846
5.000	.84745948	.78957276	.93066712	.75547633	.88606810	.83804603
6.000	.81750751	.76563076	.90003805	.73396948	.86039321	.81317014
7.000	.79449433	.74662625	.87662342	.71659555	.84018450	.79361165
8.000	.77591217	.73090595	.85777020	.70204372	.82353672	.77752157
9.000	.76038899	.71752021	.84202699	.68953955	.80938495	.76386191
10.000	.74709961	.70587728	.82852570	.67858870	.79707662	.75199761
15.000	.70000750	.66340488	.78032566	.63818988	.75202471	.70870298
20.000	.66942633	.63504872	.74860020	.61094758	.72168301	.67966050
25.000	.64688364	.61387680	.72495101	.59052711	.69885222	.65786380
30.000	.62909852	.59705695	.70612966	.57427582	.68060382	.64047367

TABLE 7. O_2 collision integrals

T^*	$\langle\Omega^{(1,1)*}\rangle$	$\langle\Omega^{(1,2)*}\rangle$	$\langle\Omega^{(2,2)*}\rangle$	$\langle\Omega^{(1,3)*}\rangle$	$\langle\Omega^{(2,3)*}\rangle$	$\langle\Omega^{(3,3)*}\rangle$
.600	1.92134797	1.56519099	2.14044483	1.34406901	1.85100009	1.71301977
.700	1.76351846	1.43752578	1.96755952	1.24470903	1.69459497	1.57595064
.800	1.63841256	1.34083820	1.82607371	1.17146515	1.57274191	1.46952356
.900	1.53792986	1.26550730	1.71195371	1.11525887	1.47753909	1.38473264
1.000	1.45520367	1.20580179	1.61641455	1.07116623	1.40086467	1.31654901
1.200	1.32903331	1.11634548	1.47129830	1.00576763	1.28712767	1.21361856
1.400	1.23755511	1.05361734	1.36550231	.95941924	1.20759817	1.14030728
1.600	1.16839183	1.00656899	1.28667449	.92458045	1.14890298	1.08579012
1.800	1.11410524	.97003071	1.22584687	.89707578	1.10403943	1.04355267
2.000	1.07112843	.94082305	1.17721554	.87462108	1.06853933	1.00984171
2.200	1.03558918	.91667111	1.13770443	.85579574	1.03962478	.98226197
2.400	1.00561735	.89623478	1.10509850	.83966828	1.01553480	.95920562
2.600	.98015835	.87866939	1.07762755	.82560480	.99508406	.93957101
2.800	.95837467	.86335585	1.05408206	.81316530	.97743474	.92258143
3.000	.93943300	.84983156	1.03363998	.80202837	.96200126	.90768211
3.200	.92263858	.83775938	1.01569968	.79196672	.94832142	.89447009
3.400	.90758429	.82687391	.99979754	.78279128	.93609782	.88263621
3.600	.89401656	.81697718	.98557177	.77436834	.92505649	.87194564
3.800	.88173149	.80790613	.97278058	.76659237	.91499845	.86221674
4.000	.87054900	.79954676	.96117574	.75936962	.90578953	.85330180
5.000	.82656511	.76558486	.91575028	.72945095	.86883768	.81751220
6.000	.79501748	.74016330	.88346697	.70650514	.84154460	.79111892
7.000	.77062650	.71993957	.85864589	.68793497	.81996318	.77028291
8.000	.75091630	.70317381	.83858996	.67236365	.80212036	.75308909
9.000	.73442121	.68887699	.82179464	.65897512	.78691200	.73845984
10.000	.72029684	.67642951	.80735055	.64724538	.77365935	.72573179
15.000	.67008196	.63097092	.75552567	.60397374	.72500285	.67916817
20.000	.63738118	.60061797	.72126660	.57483054	.69217314	.64789078
25.000	.61327239	.57797754	.69569779	.55302469	.66747674	.62442886
30.000	.59425972	.56001488	.67534837	.53570337	.64775605	.60573087